Front. Optoelectron. 2012, 5(4): 403–413
DOI 10.1007/s12200-012-0281-y

RESEARCH ARTICLE

Simple solutions for photonic power-efficient ultra-wideband system assisted by electrical bandpass filter

Jianji DONG (✉), Yuan YU, Bowen LUO, Dexiu HUANG, Xinliang ZHANG

Wuhan National Laboratory for Optoelectronics (WNLO), College of Optoelectronic Science and Engineering, Huazhong University of Science and Technology, Wuhan 430074, China

Abstract We propose and experimentally demonstrate two simple solutions for power-efficient ultra-wideband (UWB) radio frequency (RF) system assisted by an electrical bandpass filter (EBPF). In the first solution, any optical Gaussian pulse with enough bandwidth is transmitted over optical fiber link, and then converted to a power-efficient UWB pulse by an EBPF with a passband of 3.1–10.6 GHz. The transmission and modulation of UWB signal is processed in optical domain, whereas the generation of UWB is processed in electrical domain. Both UWB modulations of on-off keying (OOK) and binary phase shift keying (BPSK) are experimentally demonstrated. In the second solution, the EBPF is used to convert any electrical waveform to a power-efficient UWB pulse. Then the electrical UWB pulse is converted to an optical UWB pulse with a Mach-Zehnder modulator (MZM), and then distributed over long haul fiber link. These two solutions embody the advantages of both low-loss long-haul transmission of optical fiber and mature electrical circuits. And the millimeter-wave UWB signal is also demonstrated.

Keywords ultra-wideband (UWB), microwave photonics, pulse shaping

1 Introduction

Ultra-wideband (UWB) systems have attracted great interest in the past decade for its advantages of high data rate, low power consumption, and immunity to multipath fading in short-range wireless communications and sensor networks [1–3]. The radio frequency (RF) spectrum of UWB signals has been allocated by the U. S. Federal Communications Commission (FCC) for unlicensed use from 3.1 to 10.6 GHz frequency bands [1]. Many approaches to generating UWB signals were implemented using electronic circuits in the electrical domain, which had the advantages of low cost and easy implementation [4,5]. However, the electrical UWB pulses could only transmit within tens of meters due to the extremely low radiation power. One of the most popular methods is employing UWB-over-fiber technology, which is proposed not only to extend the area of coverage but also to offer the availability of undisrupted service across different networks [2,3]. Therefore photonic manipulation (including generation, transmission, and modulation) of UWB signals is very attractive since it can be easily incorporated into UWB-over-fiber networks [6–15]. However, the photonic UWB system is quite high cost and complex since many expensive optoelectronic devices, such as several lasers and nonlinear optical signal processors are required. Besides, even the UWB monocycle and doublet waveforms were generated in optical domain, the RF spectra of these waveforms definitely violated the standard FCC mask in global positioning system (GPS) band (0.9–1.63 GHz) until the total power are greatly attenuated [16]. However, power attenuation leads to less transmission distance in free space.

To obtain a power-efficient UWB waveform without power attenuation, some specific UWB waveforms were designed so that their RF spectral energy could be fully filled into the FCC mask with high power efficiency. One of the most popular methods is combining several temporal monocycle (as basic unit) pulses with proper delays to achieve a power-efficient UWB waveform. For example, we combined three weighted monocycles using a nonlinear semiconductor optical amplifier [17]. Zhou et al. employed a highly nonlinear fiber to generate two asymmetric monocycles, which are combined as a power-efficient UWB waveform [18,19]. Li et al. employed two phase modulators instead [20]. Abraha et al. presented a relevantly lower cost solution to combine two modified

Received July 1, 2012; accepted August 8, 2012

E-mail: jjdong@mail.hust.edu.cn

doublet pulses by a balanced photodetector (BPD) [16]. Some of these methods achieved very high power efficiency of UWB waveforms at the cost of bulky system and expensive devices. Another popular method was to design a power-efficient shape in frequency domain with an apodized fiber Bragg grating (FBG) and then employ frequency-time mapping techniques [21–23]. It is very attractive since the manipulation of frequency shape is much easier than that of time domain.

To obtain a power-efficient FCC-compliant UWB waveform, we aim to reshape any large-bandwidth signal with a passband of 3.1–10.6 GHz directly. As we know, to design an electrical bandpass filter (EBPF) is much easier than to design an optical bandpass filter in such a narrow band. So we propose several simple solutions to generate power-efficient UWB signals assisted by an EBPF. The basic concept is that the transmission and modulation of optical signal is implemented in optical domain, whereas the generation of UWB signals is processed in electrical domain. These solutions embody the advantages of both low-loss long-haul transmission of optical fiber link and mature electrical circuits. In the first solution, any optical return-to-zero (RZ) pulse with enough bandwidth is transmitted over optical fiber link, and then converted to a power-efficient UWB pulse by an EBPF with a passband of 3.1–10.6 GHz. Both UWB modulations of on-off keying (OOK) and binary phase shift keying (BPSK) are experimentally demonstrated. In the second solution, we generate an electrical power-efficient UWB waveform by the EBPF, and the UWB waveform is then converted to an optical UWB signal by a MZM.

2 First solution for UWB system

Figure 1 shows the first solution of power-efficient UWB configuration based on the hybrid of optical fiber and electrical circuits. The system consists of an optical transmission link, such as optical access network and RF/wireless transmission link, such as RF circuits and antenna. A central node generates an optical pulse (RZ signal) to the optical access network, which will be transmitted through the single mode fiber (SMF) and received by a photodetector (PD). Then an EBPF with a passband of 3.1–10.6 GHz will convert the RZ signal to a UWB RF signal for wireless transmission. The RZ optical signals can be multiplexed with time division multiplexing (TDM) or wavelength division multiplexing (WDM) in the optical access network to improve the communication capacity. As such, a de-multiplexing device, such as optical switch or arrayed waveguide grating is required accordingly before the PD. Besides, if the antenna is designed to have the same frequency response to the EBPF, then the EBPF can be removed in the system for reducing the cost. Any RZ signal with enough bandwidth (typically larger than 10 GHz) can be converted into a power-efficient electrical UWB waveform by the EBPF, because the reshaping spectrum completely complies with the FCC mask from 3.1 to 10.6 GHz, and all other frequency components are totally eliminated.

As an example, Fig. 2 shows the experimental setup of power-efficient UWB generator. First, a laser diode (LD) is followed by a MZM, which is driven by a bit pattern generator (BPG) to generate an optical RZ signal. Then, the generated RZ signal is transmitted in the SMF link, equivalent to distribution in the optical access network. As an electrical circuit, the PD and EBPF convert the optical RZ signal to a power-efficient electrical UWB signal. By changing the direct current (DC) bias voltage of the MZM, both RZ and inverted RZ pulses can be generated in the optical domain. Therefore, bi-polar UWB signals can be obtained as well, dependent on the polarity of incoming RZ signal. In our scheme, the transmission and modulation of UWB signal are processed in optical domain, whereas the generation of UWB signal is processed in electrical domain. This solution embodies the advantages of both low-loss long-haul transmission of optical fiber and low-cost mature RF circuit.

Assume that the optical RZ signal has no distortion after SMF transmission and is linearly converted to electrical RZ signal by the PD, expressed by $g(t)$. The EBPF has a frequency response function as $H(f) = u(f - f_{\text{low}}) - u(f - f_{\text{up}})$, where u denotes the unit step function and f_{low} and f_{up} are the start frequency and stop frequency of the EBPF. Applying the inverse Fourier transform, the impulse response of the EBPF can be described as $h(t) = f_{\text{BW}} \sin c(f_{\text{BW}} t) \cos(2\pi f_0 t)$, where f_{BW} and f_0 are bandwidth and central frequency of the EBPF, respectively. Therefore, the output temporal waveform of EBPF is the convolution of input RZ pulse and the EBPF impulse response, expressed by

$$E_{\text{out}}(t) = g(t) * [f_{\text{BW}} \sin c(f_{\text{BW}} t) \cos(2\pi f_0 t)]. \quad (1)$$

Equation (1) characterizes the generated UWB waveform. If the input RZ pulse is an ultrashort pulse (less than 10 ps), showing a broadband spectrum, then $g(t)$ can be regarded as a unit impulse function $\delta(t)$. Hence, the output waveform depends on the product of sin$c$ function and cosine function. Assume that f_{BW} = 7.5 GHz, and f_0 = 6.85 GHz, this means that the EBPF covers the band from 3.1 to 10.6 GHz. We simulate the output UWB waveforms and electrical spectra when changing the pulsewidth of input Gaussian pulse, as shown in Fig. 3, where Figs. 3(a)–3(c) show the input RZ pulse, EBPF output waveform, and EBPF output spectrum, respectively when the pulsewidth of Gaussian pulse is 5 ps. One can see that the output spectrum is almost a rectangle, showing a power-efficient UWB spectrum. Figures 3(d)–3(f) show the input Gaussian pulse, EBPF output waveform, and EBPF output spectrum, respectively when the pulsewidth of Gaussian pulse is 50 ps. We find that the output spectrum decreases dramatically

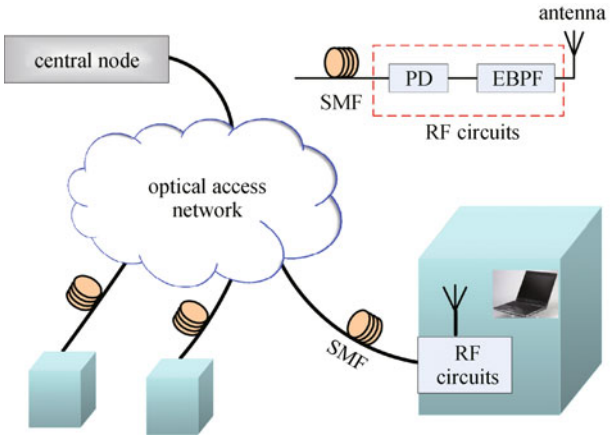

Fig. 1 First solution of power-efficient UWB configuration based on hybrid of optical fiber and electrical circuit

in the high frequencies, showing lower power efficiency. And the output waveform is also broadened largely. This is because the 50 ps RZ pulse has a narrower bandwidth. And the convolution of $g(t)$ and $h(t)$ make the output waveform vary smoothly. Therefore, both frequency and temporal characteristics are affected by the pulsewidth of RZ pulse.

Similar to Ref. [16], the spectral power efficiency (φ) is defined as the ratio between the average power of the pulse within the desired band (3.1–10.6 GHz) and the total admissible power under the FCC mask with the same band, expressed by

$$\varphi = \frac{\int_{f_{\text{low}}}^{f_{\text{up}}} Y(f)\mathrm{d}f}{\int_{f_{\text{low}}}^{f_{\text{up}}} P_{\text{FCC}}(f)\mathrm{d}f} \times 100\%, \tag{2}$$

where f_{low} = 3.1 GHz and f_{up} = 10.6 GHz, $P_{\text{FCC}}(f)$ is the FCC spectral density mask and $Y(f)$ is the power spectral density of the UWB pulse.

Based on Eq. (2), we calculate the power efficiency of generated UWB waveforms as a function of the pulsewidth of input RZ pulse, as shown in Fig. 4. The power efficiency decreases dramatically as the pulsewidth increases. If a power-efficient higher than 50% is acceptable, then the RZ pulsewidth should be narrower than 30 ps in our case. The insets of Fig. 4 are relevant temporal waveforms. One can see that the duration of UWB signals increases as the pulsewidth of RZ pulse increases. In the simulation of Ref. [21], monocycle and doublet have a power efficiency of 0.12% and 1.38%, respectively, and a power efficiency of 63.6% has been reported. The researchers of Ref. [16] proposed a high power efficiency of 57% in the simulation. However, in our case, the calculated power efficiency is as high as 97%, if the pulsewidth of RZ pulse is 5 ps.

Figure 5 shows the duration of UWB signal as a function of the EBPF bandwidth, where the central frequency of EBPF is fixed at 6.85 GHz, and the pulsewidth of RZ pulse is fixed at 25 ps. The insets are relevant temporal waveforms. One can see that the UWB duration decreases when increasing the EBPF bandwidth. This can be explained by Eq. (1). When the EBPF bandwidth increases, the sin$c$ function of Eq. (1) has a narrower temporal envelope. As a result, the UWB duration decreases as well. To transmit UWB signal with high bit rates, EBPFs with larger bandwidth are required.

For the first solution, the experimental setup is shown in Fig. 2. The LD emitted a continuous wave at a wavelength of 1560 nm. The MZM has a bandwidth of 40 GHz. The BPG generates an RZ pulse train with very low repetition rate (about 312.5 MHz). The RZ signal is transmitted by a 10 km SMF and received by a PD. A following EBPF can reshape the electrical spectrum of RZ signal to generate a power-efficient UWB pulse. The insets are corresponding measured waveforms. An electrical spectrum analyzer (Anritsu MS2668C) and a digital communications analyzer (Agilent DCA86100C) are used to measure the generated UWB signals. Two EBPF samples are designed. One of them has a passband from 3.1 to 10.6 GHz, and the other has a passband from 8 to 10 GHz. The frequency response is shown in Fig. 6. The EBPF of 8–10 GHz bandwidth shows a good bandstop feature with a frequency slope of 100 dB/GHz. Since Japan has regulated UWB band of 7.25–10.25 GHz for unlicensed use in 2008, the EBPF of 8–10 GHz may have UWB applications in Japan. We notices that the EBPF of 3.1–10.6 GHz has a small frequency slope of 22 dB/GHz in the low frequency region. This may degrade the output performance to some extent.

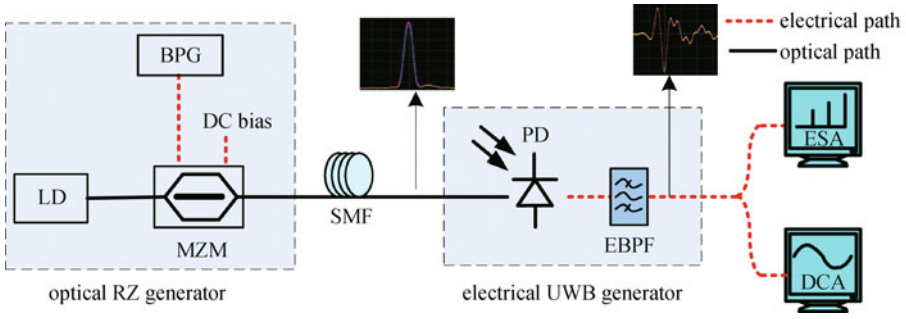

Fig. 2 Experimental setup of power-efficient UWB generator based on hybrid of optical fiber and RF circuit

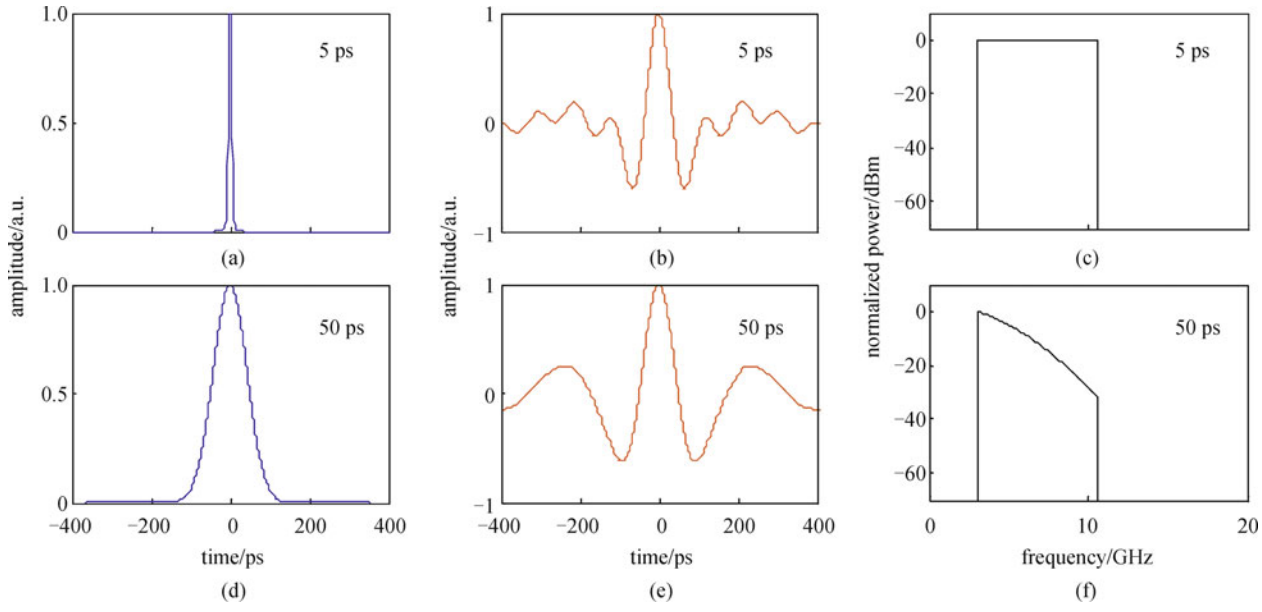

Fig. 3 (a)–(c) are input RZ pulse, EBPF output waveform, and EBPF output spectrum, respectively when the pulsewidth of Gaussian pulse is 5 ps; (d)–(f) are input Gaussian pulse, EBPF output waveform, and EBPF output spectrum, respectively when the pulsewidth of Gaussian pulse is 50 ps

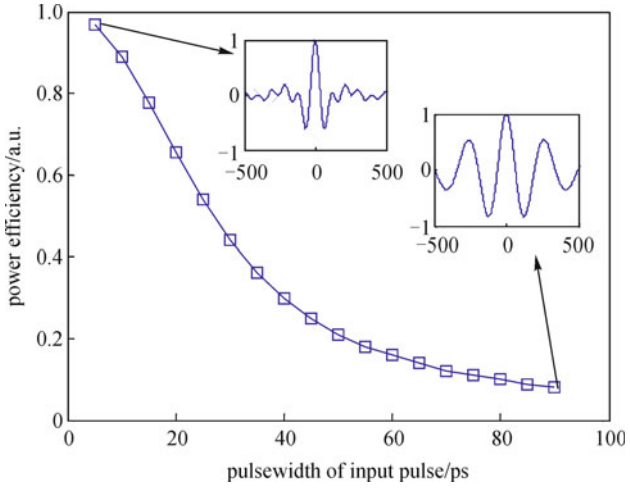

Fig. 4 Power efficiency of generated UWB waveform as function of pulsewidth of input Gaussian pulse

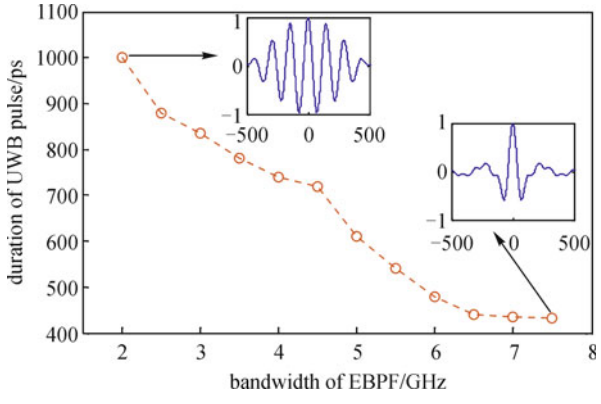

Fig. 5 Duration of UWB signal as function of EBPF bandwidth

First, an optical RZ pulse with a pulsewidth of 25 ps is generated and transmitted in the 10-km SMF. After optical to electrical conversion and filtering by the EBPF of 3.1–10.6 GHz, the power-efficient UWB waveform is measured, as shown in Fig. 7(a) and the corresponding electrical spectrum is shown in Fig. 7(b). The UWB duration is about 480 ps. We notice that the UWB waveform has some tailing ripples, which may be caused by the echo within the EBPF cavity. We also notice that the measured electrical spectrum accords with the FCC mask perfectly. The calculated power efficiency is about 53.7%. Now the pulsewidth of RZ pulses is changed to 50 ps. Another electrical UWB waveform and spectrum is observed, as shown in Figs. 7(c) and 7(d). The UWB duration is now about 570 ps with some tailing ripples. And the calculated power efficiency is 20.1%. This proves that higher power efficiency can be obtained by using narrower RZ pulse injection. From Figs. 7(b) and 7(d), we can see the UWB spectra match FCC mask perfectly without any violation in the GPS band.

To demonstrate UWB pulse amplitude modulation (PAM), the input RZ clock train is modulated at 2.5 Gbit/s and the RZ pulsewidth is set at 50 ps. The measured UWB waveform and spectrum are shown in Figs. 8(a) and 8(b), respectively. Similarly, we can see the UWB spectra match FCC mask perfectly without any violation in the GPS band.

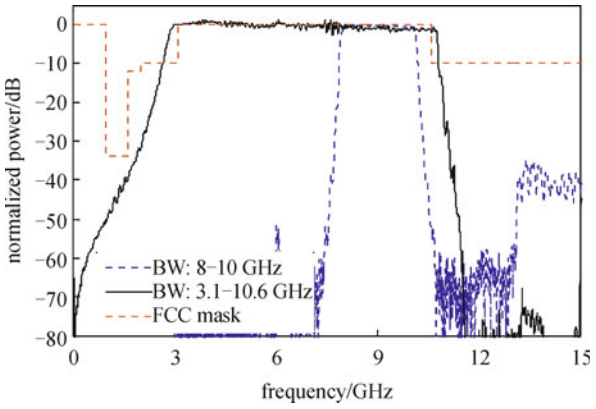

Fig. 6 Frequency response of two EBPF samples

To investigate the impact of EBPF bandwidth on the UWB waveform, the EBPF of 8–10 GHz is employed. Figures 9(a) and 9(c) show the measured UWB waveforms using an EBPF of 8–10GHz bandwidth with 25 ps and 50 ps RZ pulse injection, respectively. The UWB duration is about 720 and 900 ps, respectively. Figures 9(b) and 9(d) are the corresponding electrical spectra. One can see that the spectra exactly cover the band of 8–10 GHz and comply with the FCC mask as well. And the UWB spectrum with 25 ps RZ injection shows a higher power-efficiency than that with 50 ps RZ injection.

Since both RZ and inverted RZ pulses can be generated in optical domain, the generated UWB signals can be modulated with BPSK, which gives extra 3 dB improvement in signal-noise ratio (SNR) for any given noise level. Figure 10 gives an example for BPSK modulation of UWB signals. Two parallel LDs are modulated by two MZMs to generate RZ signals and inverted RZ signals, respectively. Both RZ pulse and inverted RZ pulse have a pulsewidth of 50 ps. These two beams are coupled with one delayed properly. Finally, the UWB BPSK modulation could be obtained after PD detection and filtering of the EBPF. The BPSK modulation of UWB signals can be used for multi-user communication, such as code division multiple access (CDMA) technology. We select Walsh-Hadamard codes as the orthogonal codes in our experiment. As for a code length of 4, the four orthogonal codes are $\{(C1,C2,C3,C4)\} = \{(1,1,1,1), (1,1,-1,-1), (1,-1,1,-1), (1,-1,-1,1)\}$. Figures 11(a)–11(d) show the measured four orthogonal codes with UWB sequences. The pulse duration of each code is about 2.0 ns. And Figs. 11(e)–11(h) show the corresponding RF spectra, respectively, which indicate that the generated signals in the frequency domain fit well within the FCC mask. These orthogonal codes can individually serve as signature codes for different communication users. It should be noted that the dispersion management is required since these CDMA codes are formed by two different wavelengths.

3 Second solution for power-efficient UWB generation

In the second solution, the EBPF is used to reshape an electrical signal to a power efficient UWB signal and then modulate it onto an optical carrier to form an optical UWB

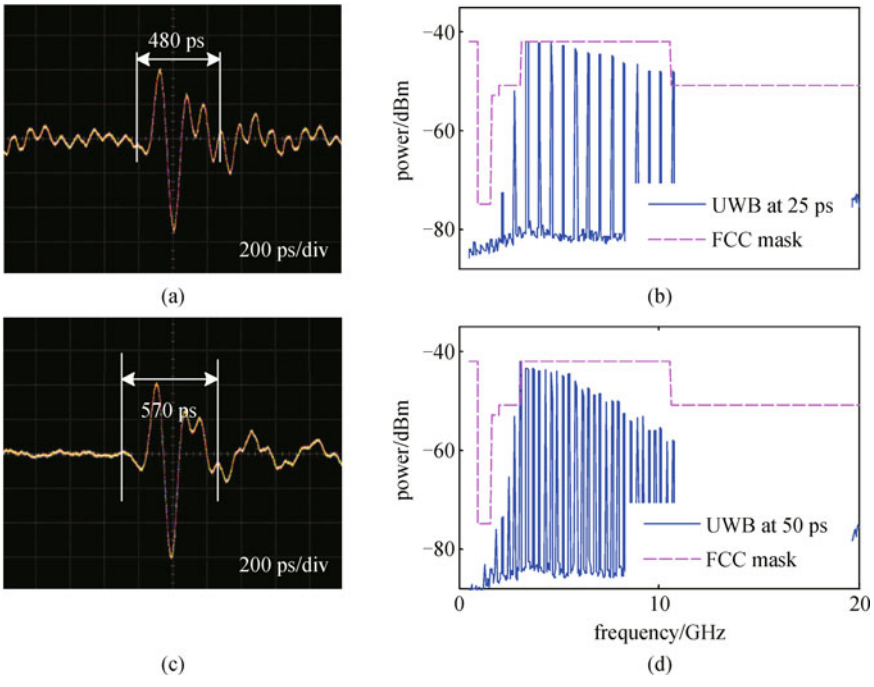

Fig. 7 (a) and (b) are measured UWB waveform and electrical spectrum with 25 ps RZ pulse injection; (c) and (d) are measured UWB waveform and electrical spectrum with 50 ps RZ pulse injection

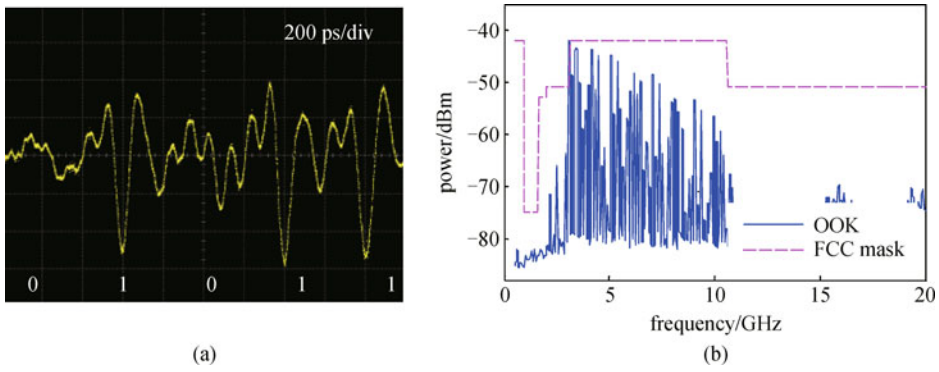

Fig. 8 (a) and (b) are measured PAM of UWB signals and its electrical spectrum with 50 ps RZ pulse injection

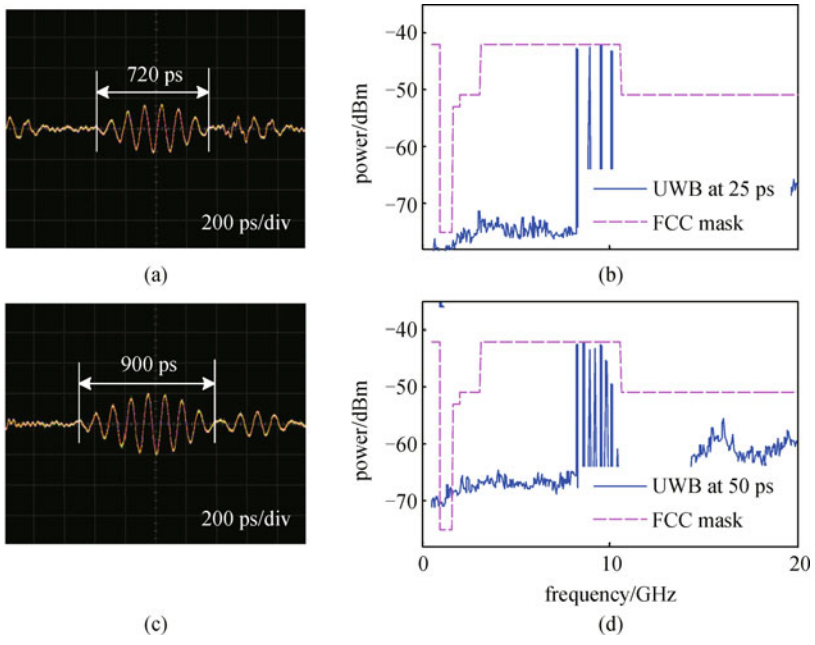

Fig. 9 (a) and (b) are measured UWB waveform and electrical spectrum with 25 ps RZ pulse injection; (c) and (d) are measured UWB waveform and electrical spectrum with 50 ps RZ pulse injection. An EBPF of 8–10 GHz is used

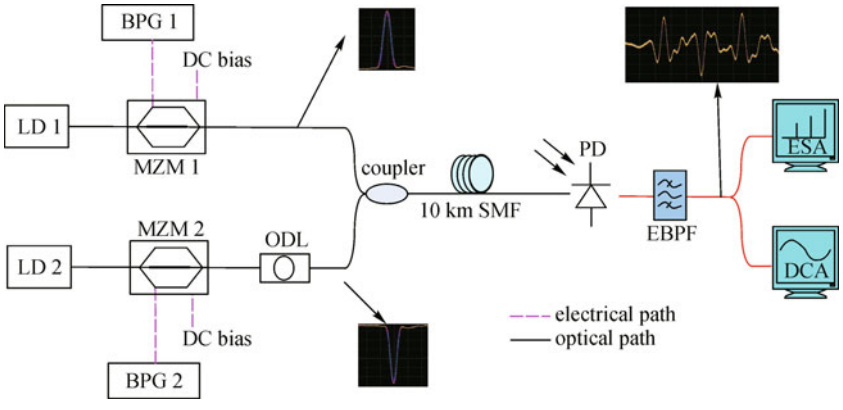

Fig. 10 Experimental setup for BPSK modulation of UWB signals

signal. The experimental setup is shown in Fig. 12. First, a BPG generates an arbitrary waveform with enough bandwidth (typically larger than 10 GHz). Consequently, an EBPF is used to extract the electrical spectrum of input pulse with a passband of 3.1–10.6 GHz. Thus, the output electrical waveform should be a power-efficient UWB signal since its spectrum completely complies with the FCC mask from 3.1 to 10.6 GHz, and all other frequency components are totally eliminated. A LD generates a continuous wave, which is intensity-modulated by the power-efficient UWB electrical signal. Finally, a power-efficient photonic UWB pulse is generated when the intensity modulator, such as MZM is set at the linear transmission region. By changing the DC bias voltage to the positive or negative transmission region of the MZM, a pair of polarity-reversed UWB signals can be obtained. The photonic UWB signal then can be distributed by the SMF for a long distance, and received by a PD. The photonic UWB pulse in our scheme shows a good tolerance to the fiber dispersion due to its single optical carrier. And the UWB RF spectrum completely complies with the FCC mask because of the frequency reshaping of the EBPF.

First, a Gaussian pulse with a pulsewidth of 50 ps is generated from the BPG. By adjusting the DC bias of the MZM, we observe a pair of polarity-reserved photonic UWB pulses, as shown in Figs. 13(a) and 13(b), respectively. The corresponding electrical spectra are shown in Figs. 13(e) and 13(f). The durations of UWB waveforms are about 580 ps. We notice that these UWB waveforms have some tailing ripples, which may be also caused by the echo within the EBPF cavity. The measured electrical spectra have a little overflow in the GPS band. The mean reason lies in the imperfect modulation characteristics of MZM. The overflow of GPS band can

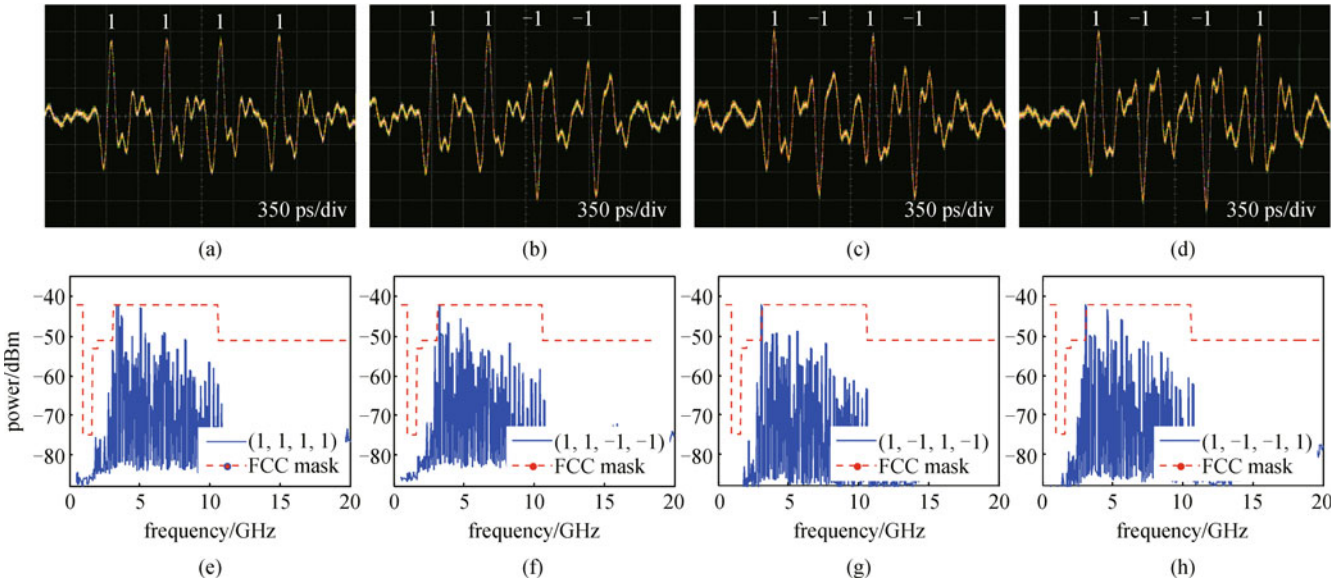

Fig. 11 (a)–(d) are generated temporal waveforms of 4-bit Walsh-Hadamard codes; (e)–(h) are electrical spectra, respectively

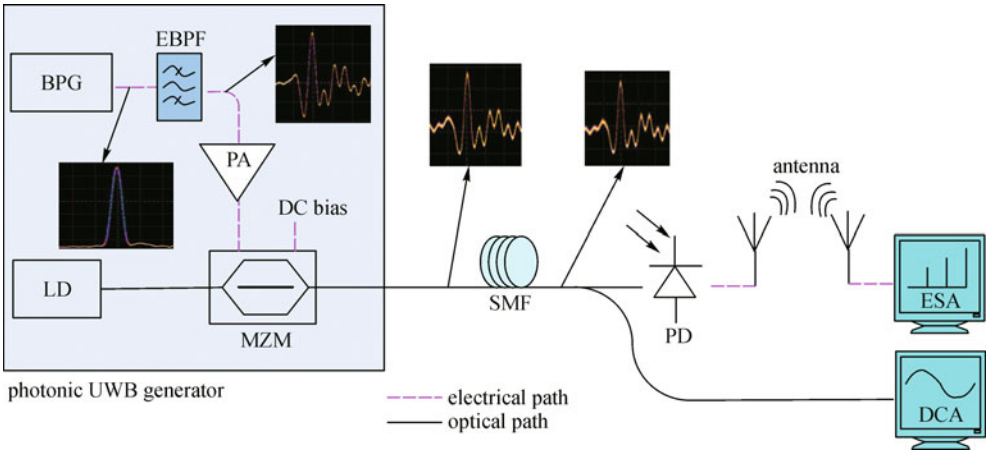

Fig. 12 Second solution of power-efficient UWB generation and transmission

be easily eliminated by designing an EBPF with a better bandstop feature. The calculated power efficiency of Figs. 13(e) and 13(f) is 27.6% and 28%, respectively. Now the pulsewidth of Gaussian pulses is changed to 25 ps. Another pair of polarity-reversed UWB waveforms is measured, as shown in Figs. 13(c) and 13(d). The UWB duration is now about 550 ps with some tailing ripples. The corresponding electrical spectra are shown in Figs. 13(g) and 13(h), where the calculated power efficiency is 57.6% and 53%, respectively. This proves that higher power efficiency can be obtained by using narrower Gaussian pulse injection.

Here, the pulsewidth of Gaussian pulses is fixed at 25 ps. To investigate the transmission characteristics of photonic UWB signals, Figs. 14(a) and 14(b) show measured UWB waveforms after transmission by 10 km SMF. One can see the waveforms resemble the UWB waveforms before transmission. The UWB duration remains 550 ps. Figures 14(c) and 14(d) are the corresponding electrical spectra with high power efficiency. This proves that our scheme has a large tolerance to the fiber dispersion. This is because the MZM operates under push-pull state and generated UWB pulses are chirp-free.

The UWB wireless transmission after SMF is also studied. The frequency responses of the UWB antenna pair with a distance of 1, 5, 10, and 20 cm are shown in Fig. 15. It can be observed that the UWB antenna pair exhibits a bandpass character and the 10 dB bandwidth is about 10 GHz (from 4 to about 14 GHz). A larger distance leads to a higher insertion loss. In the experiment, the UWB antennas are placed in their peak radiation direction in the azimuth plane with a distance of 5 cm. The received UWB waveform and spectrum are shown in Figs. 16(a) and 16(b), respectively. The waveform has some distortion but the spectrum is still FCC-compliant.

Finally, the millimeter-wave UWB signal is also investigated. We use another MZM, which operates at the carrier suppression modulation. The input RF source is a clock of 10 GHz. Thus, the original UWB signal is modulated to a millimeter-wave UWB signal at 20 GHz. Figures 17(a) and 17(c) show a pair of polarity-reversed millimeter wave UWB signals. Figures 17(b) and 17(d) are the correspondingly measured RF spectra. From the spectra, one can see the UWB spectra have a 10 dB bandwidth from 22.3 to 27.5 GHz, which is also for unlicensed use.

These two solutions of power-efficient UWB generation show very simple structure and high stability since only one laser, one EBPF, and one intensity modulator are required. Comparing to the scheme of waveform combination of basic UWB units [17–19], these schemes are simpler and more stable. Comparing to frequency-time mapping techniques [21–23], these schemes are more robust and simpler, since the high-resolution filtering in electoral circuits is much easier than in optical filtering devices. Comparing these two solutions, we find that the first solution is a scheme of electrical UWB generation, and the RF spectrum accords with the FCC mask perfectly. The second solution is a scheme of optical UWB generation, but the RF spectrum still slightly violates the GPS band. The optical UWB waveform can be distributed in the fiber link for long haul. While the electrical UWB waveform should be loaded onto an optical carrier before being distributed in the fiber link. Besides, the first solution is stricter with the modulator than the second one since high speed RZ pulses are distributed over the fiber link. While in the second solution, the MZM with a bandwidth of 10.6 GHz is enough.

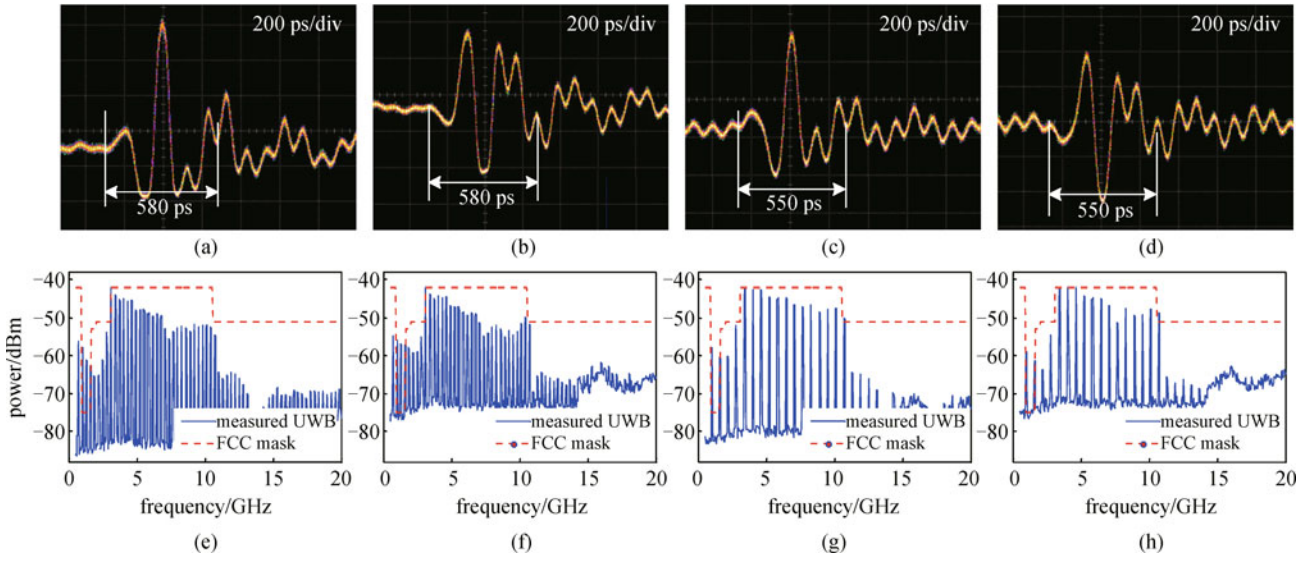

Fig. 13 (a)–(b) are pair of measured bi-polar UWB waveforms with 50 ps Gaussian pulse injection; (c)–(d) are pair of measured bi-polar UWB waveforms with 25 ps Gaussian pulse injection; (e)–(h) are corresponding electrical spectra, respectively

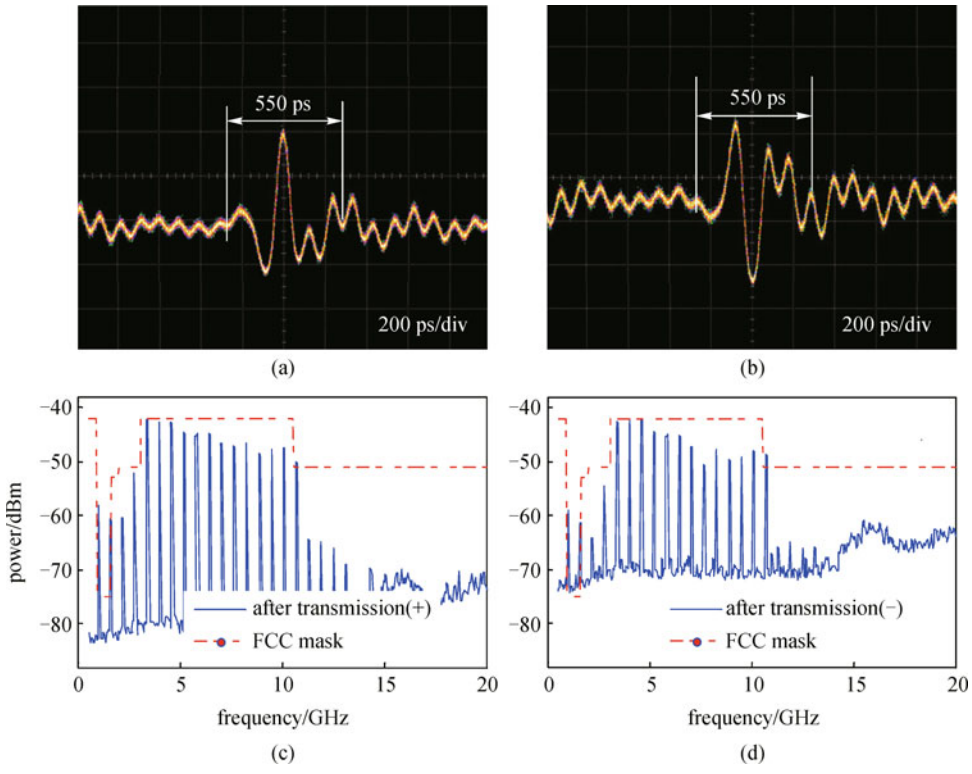

Fig. 14 (a) and (b) are pair of polarity-reversed UWB waveforms after transmission by 10 km SMF; (c) and (d) are corresponding electrical spectra

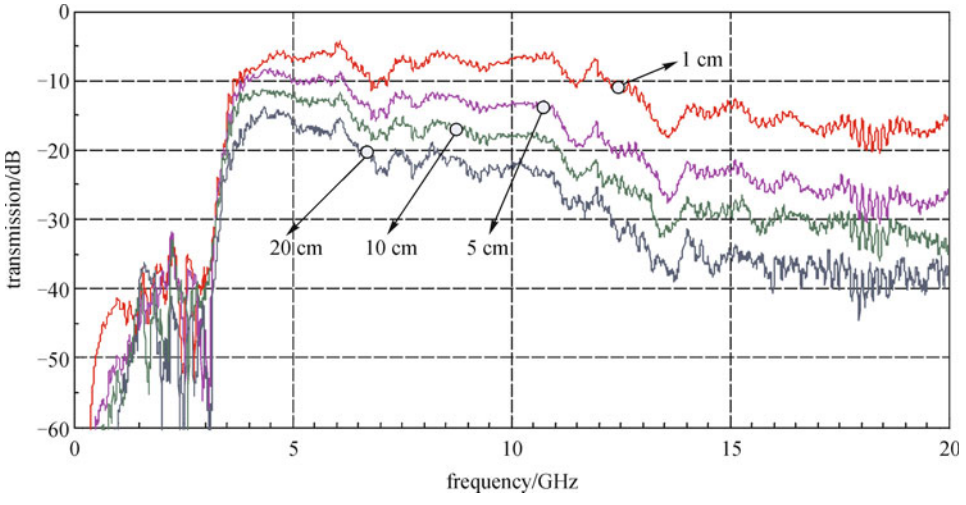

Fig. 15 Frequency responses of UWB antenna pair in their peak radiation direction in azimuth plane with distance of 1, 5, 10, and 20 cm, respectively

4 Conclusions

In summary, two simple solutions are proposed to generate power-efficient UWB RF signal based on the hybrid of optical fiber and RF circuits. The basic idea is that an EBPF is used to reshape any large bandwidth signal to a power-efficient UWB signal. In the first solution, any optical RZ pulse with enough bandwidth is transmitted over optical fiber link, and then converted to a power-efficient UWB pulse by an EBPF with a passband of 3.1–10.6 GHz. In the second solution, an electrical power-efficient UWB waveform is generated by the EBPF, and then loaded onto an optical carrier to form a power-efficient UWB signal by an MZM. Finally, the optical UWB signal is transmitted over the fiber link. These solutions embody the advantages of both low-loss long-haul transmission of optical fiber link

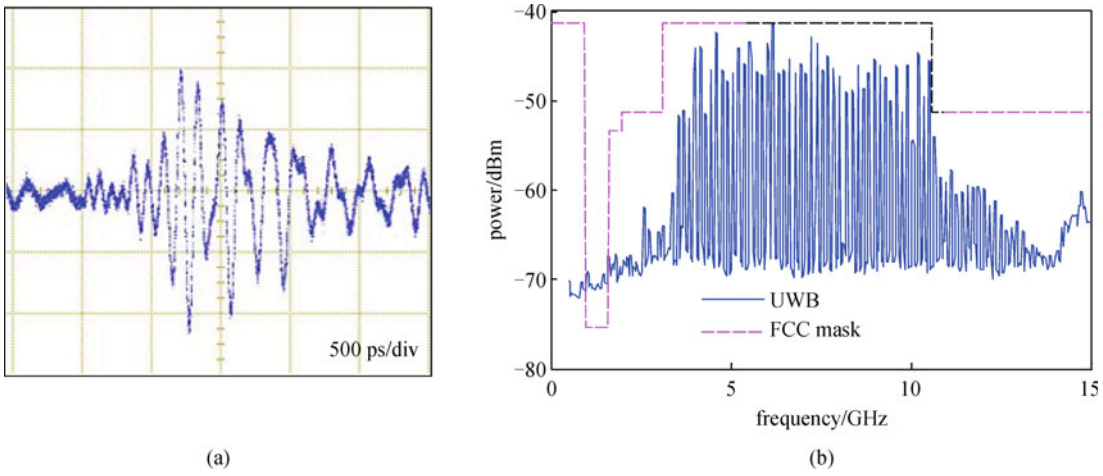

Fig. 16 Measured waveform (a) and RF spectrum (b) after antenna transmission

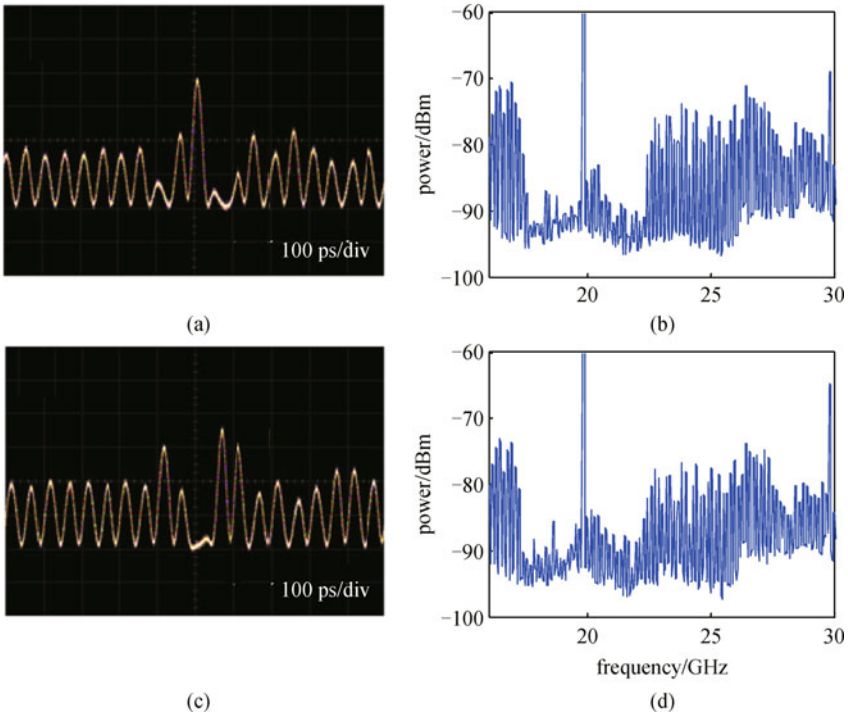

Fig. 17 (a) and (c) are pair of polarity-reversed millimeter wave UWB signals; (b) and (d) are correspondingly measured RF spectra

and mature RF circuits. The optical UWB pulse shows a good tolerance to the fiber dispersion.

Acknowledgements This work was partially supported by the National Basic Research Program of China (No. 2011CB301704), the Program for New Century Excellent Talents in Ministry of Education of China (No. NCET-11-0168), and the National Natural Science Foundation of China (Grant Nos. 60901006 and 11174096).

References

1. Porcino D, Hirt W. Ultra-wideband radio technology: potential and challenges ahead. IEEE Communications Magazine, 2003, 41(7): 66–74
2. Yao J. Photonics for ultrawideband communications. IEEE Microwave Magazine, 2009, 10(4): 82–95
3. Ran M, Lembrikov B I, Ben Ezra Y. Ultra-wideband radio-over-optical fiber concepts, technologies and applications. IEEE Photonics Journal, 2010, 2(1): 36–48
4. Kim H, Park D, Joo Y. All-digital low-power CMOS pulse generator for UWB system. Electronics Letters, 2004, 40(24): 1534–1535
5. Bachelet Y, Bourdel S, Gaubert J, Bas G, Chalopin H. Fully integrated CMOS UWB pulse generator. Electronics Letters, 2006, 42(22): 1277–1278
6. Zheng J Y, Zhang M J, Wang A B, Wang Y C. Photonic generation

of ultrawideband pulse using semiconductor laser with optical feedback. Optics Letters, 2010, 35(11): 1734–1736

7. Pan S, Yao J. UWB-over-fiber communications: modulation and transmission. Journal of Lightwave Technology, 2010, 28(16): 2445–2455
8. Yu X, Gibbon T B, Monroy I T. Experimental demonstration of all-optical 781.25-Mb/s binary phase-coded UWB signal generation and transmission. IEEE Photonics Technology Letters, 2009, 21 (17): 1235–1237
9. Yu X, Braidwood Gibbon T, Pawlik M, Blaaberg S, Tafur Monroy I. A photonic ultra-wideband pulse generator based on relaxation oscillations of a semiconductor laser. Optics Express, 2009, 17(12): 9680–9687
10. Wang F, Dong J, Xu E, Zhang X. All-optical UWB generation and modulation using SOA-XPM effect and DWDM-based multi-channel frequency discrimination. Optics Express, 2010, 18(24): 24588–24594
11. Dong J, Zhang X, Xu J, Huang D, Fu S, Shum P. Ultrawideband monocycle generation using cross-phase modulation in a semiconductor optical amplifier. Optics Letters, 2007, 32(10): 1223–1225
12. Wang S, Chen H, Xin M, Chen M, Xie S. Optical ultra-wide-band pulse bipolar and shape modulation based on a symmetric PM-IM conversion architecture. Optics Letters, 2009, 34(20): 3092–3094
13. Wang Q, Yao J. Approach to all-optical bipolar direct-sequence ultrawideband coding. Optics Letters, 2008, 33(9): 1017–1019
14. Dai Y, Yao J. High-chip-count UWB bi-phase coding for multi-user UWB-over-fiber system. Journal of Lightwave Technology, 2009, 27(11): 1448–1453
15. Yu Y, Dong J, Li X, Zhang X. UWB monocycle generation and bi-phase modulation based on mach-zehnder modulator and semiconductor optical amplifier. Photonics Journal, 2012, 4(2): 327–339
16. Abraha S T, Okonkwo C M, Tangdiongga E, Koonen A M J. Power-efficient impulse radio ultrawideband pulse generator based on the linear sum of modified doublet pulses. Optics Letters, 2011, 36(12): 2363–2365
17. Dong J, Luo B W, Huang D, Zhang X. Photonic generation of power-efficient FCC-compliant ultra-wideband waveforms using (SOA): theoretical analysis and experiment verifications. Chinese Physics B, 2012, 21(4): 043201
18. Xu X, Zhou E B, Liang Y, Yuk T I, Lui K S, Wong K K Y. Power-efficient photonic BPSK coded ultrawideband signal generation. In: Proceedings of OFC/NFOEC, 2011, OTuF5
19. Zhou E B, Xu X, Liu K S, Wong K K Y. A power-efficient ultra-wideband pulse generator based on multiple PM-IM conversions. IEEE photonics Technology Letters, 2010, 22(14): 1063–1065
20. Li P, Chen H, Chen M, Xie S. A power-efficient photonic OOK and BPSK modulated Gigabit/s IR-UWB over fiber system. In: Asia-Pacific, MWP/APMP Singapore, 2011, 254–257
21. Abtahi M, Dastmalchi M, LaRochelle S, Rusch L A. Generation of arbitrary UWB waveforms by spectral pulse shaping and thermally-controlled apodized FBGs. Journal of Lightwave Technology, 2009, 27(23): 5276–5283
22. Abtahi M, Mirshafiei M, LaRochelle S, Rusch L A. All-optical 500-Mb/s UWB transceiver: an experimental demonstration. Journal of Lightwave Technology, 2008, 26(15): 2795–2802
23. Abtahi M, Magné J, Mirshafiei M, Rusch L A, LaRochelle S. Generation of power-efficient FCC-compliant UWB waveforms using FBGs: analysis and experiment. Journal of Lightwave Technology, 2008, 26(5): 628–635